BOR DERGİSİ
JOURNAL OF BORON
http://dergipark.gov.tr/boron

Alternating current electrophoretic deposition of HA and hBN nanoparticles on Ti substrate

Merve Geçgin[1*], Yapıncak Göncü[2], Nuran Ay[3]

[1]Department of Material Science and Engineering, Anadolu University, Eskişehir, Turkey, ORCID ID orcd.org/0000-0002-9674-9168
[2]BORTEK Boron Technologies and Mechatronics Inc., Eskişehir, Turkey, ORCID ID orcd.org/0000-0002-8602-9765
[1]Department of Material Science and Engineering, Anadolu University, Eskişehir, Turkey, ORCID ID orcd.org/0000-0002-2228-9904

ARTICLE INFO

Article history:
Received 1 March 2017
Received in revised form 13 September 2017
Accepted 14 September 2017
Available online 25 September 2017

Research Article

Keywords:
Alternating current electrophoretic deposition,
Hexagonal boron nitride,
Hydroxyapatite,
Composite coating

ABSTRACT

Hydroxyapatite (HA) and hexagonal boron nitride (hBN) are biocompatible materials. In this study, nano HA and nano hBN particles were used for coatings on titanium (Ti) substrate. The nanoparticles were deposited on Ti substrates by alternating current electrophoretic deposition (AC-EPD). Suspensions were consist of nano HA and also comprised of the various amount of nano hBN (0.0-2.0-5.0-10.0 and 25.0 wt% by the percentage of hydroxyapatite). The coated samples were heat treated at 800 °C in Ar atmosphere for 2 hours. Sintered samples were characterized by XRD and SEM-EDS. Coating thickness was measured and adhesion tests (ASTM D3359–09-B) were performed. The results showed that nano HA and nano hBN composite coating with the AC-EPD method is homogeneous and crack free. It is determined that the amount of hBN in composite affects the adhesion behavior and the thickness of the coating.

1. Introduction

Hydroxyapatite is widely used as a biomaterial because of its good biocompatible, bioactive and chemically similar to inorganic compound of human skeleton system [1]. Its usage is restricted in the bone and teeth implants because of its poor mechanical properties under load bearing applications [2]. Metal based composites are developed to improve the mechanical properties of HA and several coating techniques such as dip coating [3], plasma spray [4], biomimetic [5] and electrophoretic deposition [6] are used. Among these coating techniques, electrophoretic deposition (EPD) has some advantages compared with other techniques, such as simplicity in set up, low equipment cost, the ability to coat complex shape, control of deposition thickness. Charged colloidal particles in a suspension are deposited onto an oppositely charged substrate via AC and/or DC field. While particles flow in one direction in DC, particles flow is constantly changing direction in AC from negative to positive vice versa [7-10]. Kolath et.al indicated that obtaining denser and uniform coating possible via AC-EPD(10).

Hexagonal boron nitride (hBN) is an artificial material with the layered crystal structure that has biocompatible and non-cytotoxic material for orthopedic applications [11-14]. In our previous work, hBN and HA were successfully deposited on Ti surface with uniform, crack-free coating by DC-EPD [15]. hBN improves the mechanical properties of HA [16,17] and recent studies, indicate that hBN-HA composites were used in the medical application and it was determined that it is the important contribution on bone tissue healing[18-21]. Ferah (2015) indicated that hBN containing coating decreases healing period, prevents infection and it can be utilized in the patient who has the risk of osteomyelitis[22].

Atilla et.al. demonstrated that the use of hBN in HA ceramic composite did not change the stability of the implant and increasing concentration of hBN in the composition did not cause a difference in serum boron level [23]. In this study, nano HA-nano hBN composite coatings on Ti substrate by AC-EPD were investigated.

2. Materials and methods

Nano HA powder was provided by NANOTECH Ltd., Eskişehir-Turkey, while nano hBN powder was supplied by BORTEK Inc., Eskişehir-Turkey. It was reported our previous study that HA powder included in ~10% TCP phase and highly crystalline hBN is 98% pure and the average particle size is 120 nm [24]. Commercial

*Corresponding author: mervegecgin@anadolu.edu.tr

pure titanium sheet 30x10x1.5 mm dimensions were utilized as a substrate. Each substrate was polished using SiC papers, washed and ultrasonically cleaned.

Composite suspensions were made of 1 wt. % nano HA and also comprised of various amount of nano hBN (0.0-2.0-5.0-10.0 and 25.0 wt.% nano hBN by the percentage of hydroxyapatite). Samples were coded as AC-HB 0.0, AC-HB 2.0, AC-HB 5.0, AC-HB 10.0 and AC-HB 25.0 respectively. Before deposition, N, N–dimethylformamide (10%v DMF-Merck) were added to provide strength and crack-proof improvement. The pH values of suspensions were adjusted to 4.

The experimental set up was shown in Figure 1. Ti plates were used as working and counter electrodes. Experimental studies were conducted by forming the asymmetric wave pattern. 50 Hz using under AC (Keysight, DSO1072B 70 MHz Digital oscilloscope, Agilent 33500B series Waveform generator, Agilent 33502A Amplifier) were utilized. The distance between the electrodes were 5 mm. AC-HB 0.0 samples were coated at 15 Vpp (5, 10 and 20 min), 20 Vpp (1,2,3,4 and 5 min) and 25 Vpp (1,2,3,4 and 5 min) and the other samples were coated at 25 Vpp and 2 minutes. All the samples were heat treated in laboratory tube furnace at 800 °C for 2 h in argon atmosphere.

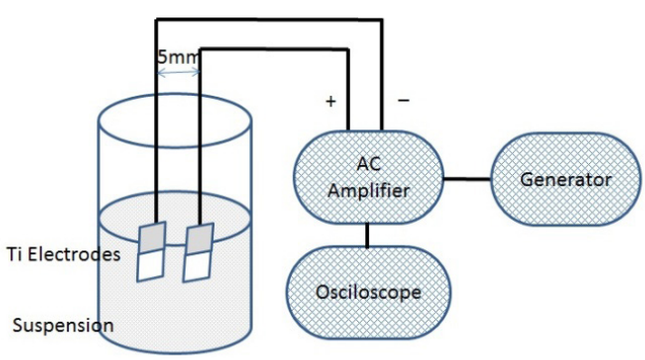

Figure 1. Experimental setup.

The coating thickness of the samples was measured by EBAN 4000 coating thickness meter. The adhesion was classified according to ASTM D3359-09 cross-cut tape-test (B) [25]. X-Ray powder diffraction patterns were obtained with a Rigaku Rint 2000 X-ray diffractometer with Cu Kα radiation (λ=1.5418 Å), in the 2θ range of 20-80° with the scan speed of 2°/min.

The amounts of the phases of all coated samples were analyzed by using JADE software and Maud program. The microstructure of deposit layers and adhesion test samples were investigated by means of scanning electron microscopy (SEM, ZEISS SUPRA 50VP) and the chemical analysis of microstructures was done with an Energy Dispersive Spectrometer (EDS-Oxford Instrument).

3. Results and discussion

Figure 2 shows the thickness of AC-HB 0.0 coated samples which was obtained under constant voltage 15 Vpp and various time by the AC-EPD method. In order to obtain a good quality coating under 15 Vpp, the minimum necessary deposition time is 5 min (Figure 2). The thickness of AC-HB 0.0 coated samples is increasing with extended time, linearly. The thickness value reached up to ~45 µm when the deposition time was 20 min under 15 Vpp. The tendency of deposited thickness vs. time in AC-EPD for HA coatings was reported [10, 26]. Kollath et al. declared that the thickness of the HA coatings by AC-EPD was increased with extended time duration (100V-30 sec=5 micron and 100 V-60 sec=22 micron) [10]. Also, Chávez-Valdez et al. indicated that the deposition yields were increased linearly with increasing deposition time (1, 3 and 5 min) at each applied voltage (5V, 10V and 20V) [26]. This study showed that the linear growth was carried out deposition time.

Figure 3 shows the thickness of AC-HB 0.0 coated samples which was obtained under 20 Vpp and 25 Vpp by AC-EPD. The thickness of AC-HB 0.0 coated samples, at 20 Vpp increased linearly and at 25 Vpp increased parabolic up to 4 min and then the thickness of the samples reached up to the constant value. Gardeshzadeh et. al. indicated that coated SnO_2 nanoparticles by AC-EPD and deposition yield was gained linearly in the beginning of deposition (to 20 min) at constant applied voltage but the rate of deposit yield were decreased with prolonged time [27]. The reason for this trend is formation of insulating layer of ceramic particles on the electrode surface [6,9,28,29]. The thickness of AC HB 0.0 for various voltages as seen Fig. 3 and Fig. 4 reaches up to the higher value with rising applied voltage for less deposition time.

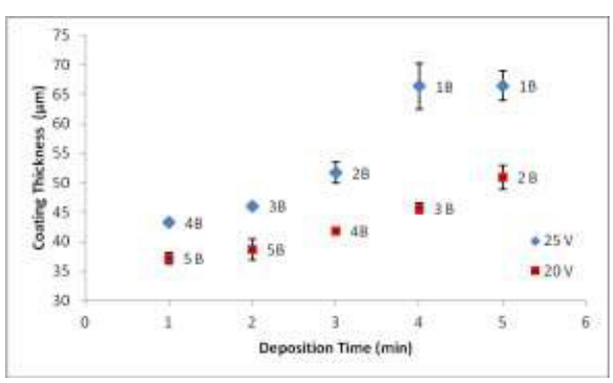

Figure 2. Coating thickness and adhesion classification of AC-HB 0.0 samples versus deposition time at 15 Vpp.

There are several test methods to determine coating quality. The available standards are: ASTM C633 and F1147 for tensile strength testing [30,31], ASTM D4501 and F1044 for shear strength testing [32,33]

and tape test (ASTM D3359 [34-36]. All samples were classified according to tape test standard (5B for 0% removal of coating, 4B for <5% removal, 3B for 5-10%, 2B for 15-35%, 1B for 35-65% and 0B for>65%). This observation leads to the conclusion that the adhesion classification of coatings for each AC-HB 0.0 samples (Fig. 2 and Fig. 3) decreases with the extended of time duration correspondingly with an increase coating thickness. As a result of this study, it is clear that there was an adhesion classification depending on the thickness such as 5B<~40 μm, 40 μm <4B<45 μm, 45 μm <3B<50 μm, 50 μm <2B<66 μm, 1B>66 μm.

The effect of applied voltage on the thickness for AC-HB 0.0 coated samples was examined at constant deposition time (5 min) (Figure 4). Increasing of applied voltage escalated the thickness linearly. It can be explained with Hamaker equation (Eq.1) [28].

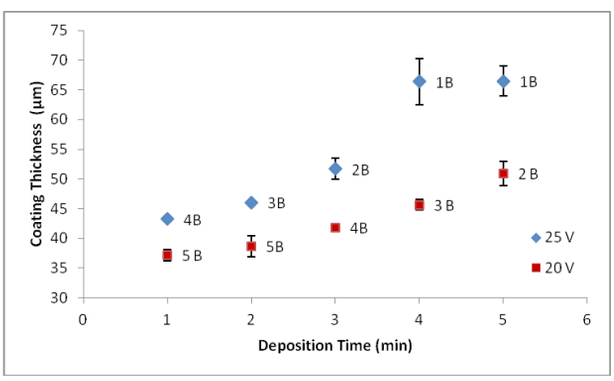

Figure 3. Coating thickness and adhesion classification of AC-HB 0.0 samples versus deposition time at 20 Vpp and 25 Vpp.

According to the equation, relation between the deposit weight, m (g) and electric field intensity/strength, E (V cm^{-1}) is:

$$m = C_s \mu \, SE \, t \qquad (1)$$

Where μ (cm^2 s^{-1} V^{-1}) is electrophoretic mobility, S (cm^2) is the surface area of the electrode, C_s (g cm^{-3}) is the concentration of the suspension and t (s) is time.

The Eq. 2 can be used instead of deposited mass [28],

$$m = SC_d \qquad (2)$$

Combining Eq. 1 and 2 gives:

$$\delta = (C_s/C_d)\, \mu E\, t \qquad (3)$$

When (C_s/C_d) *considered constant value* therefore Eq. 3 is expressed by

$$\delta = \mu E\, t \qquad (4)$$

According to Eq. 4, thickness depends on particle mobility, time and the applied electric field. In our experiments, AC-EPD were performed at 5 min and varies voltages. Due to using the same suspension for all coatings, particle mobility can be considered constant. Moreover, the electric field is constant between the electrodes, so the relation between m and E is linear. When the distance between the electrodes is constant, the electric field intensity only varies with the voltage of electric field. Therefore, the voltage can be used instead of the electric field intensity. Considered Eq. 4 and voltage effect on the thickness, the relation between them can be defined linearly.

It can be estimated that desired adhesion classification is controlled by the coating thickness in complying with various voltage-time combinations.

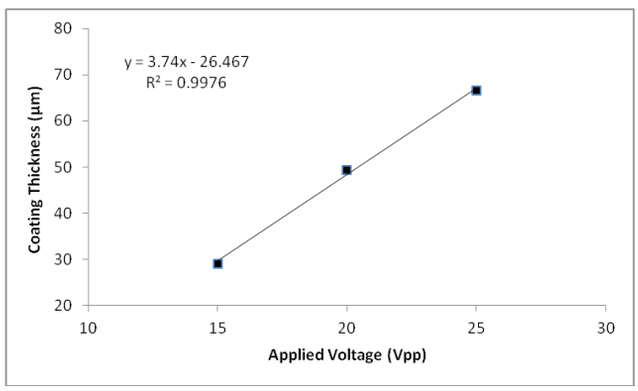

Figure 4. Coating thickness of AC-HB 0.0 samples versus applied voltage (deposition time: 5 minutes).

AC-HB 0.0 coated samples were done at 25 Vpp for 2 min and classified as 3B. Using this data, various amount of hBN in samples were investigated to obtain how the effect on coating thickness and adhesion. All composite coatings were performed at 25 Vpp for 2 min by AC-EPD and compared with AC-HB 0.0 coated by the same conditions.

It is observed that all samples are uniform and crack free at 25 Vpp and 2min. The XRD pattern of sintered composite coating samples is shown in Figure 5. Phase analysis revealed that all major peaks of HA (JCPDS PDF No: 009-0432) were present for all the samples. hBN (JCPDS PDF No: 034-421), β-TCP (JCPDS PDF No: 009-0169), TiO_2 (Rutile, JCPDS PDF No: 021-1276) and Ti (JCPDS PDF No: 044-1294) phases are detected. Beta TCP phase comes from raw nano HA powder. Rutile phase is formed as an interface phase between the substrate and coating during sintering. Kollath et. al. also observed the rutile phase as an interphase between HA and Ti substrate in the XRD spectrum of HA coatings by AC-EPD and DC-EPD after sintering at 900°C for 2 hours in high purity argon atmosphere [10]. Moreover, forming metal oxide phase between HA and Ti substrate for producing HA coatings by DC-EPD during sintering was observed other investigators [37,38].

The phase analysis results of nano HA and nano hBN phases in AC-HB 5.0, AC-HB 10.0 and AC-HB 25.0

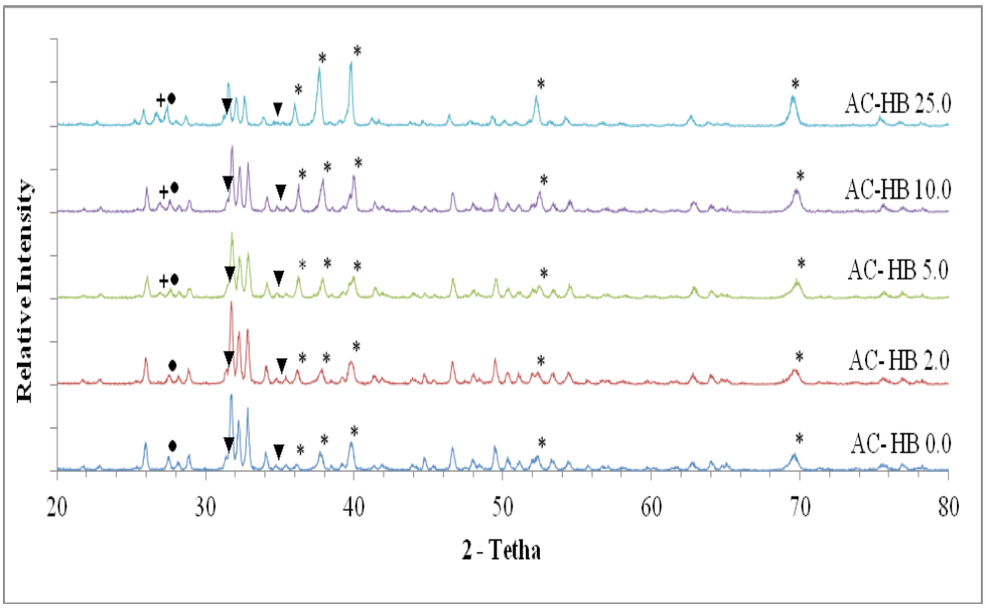

Figure 5. X-ray diffraction patterns of HA-hBN composite samples (+: hBN, ●: Rutile (TiO_2), ▼: β-TCP, *: Ti).

samples at 25 Vpp for 2 min are given Table 1. The calculations are in accordance with the amount of hBN in prepared suspensions but the amount of hBN in deposition is slightly higher. The error in this calculation is expected from mathematical calculations during Rietveld Analysis.

Table 1. Rietveld analysis results for calculated percentage of the phases present in samples.

(%)	AC-HB 5.0	AC-HB 10.0	AC-HB 25.0
HA	94.61	87.63	73.00
hBN	5.38	12.36	27.00

The coating thickness and the adhesion classification of samples are shown in Figure 6. The coating thickness decreases with increasing hBN content. It might be that there are two reasons for thickness decreasing. The first reason might be related to decreasing particle mobility in the suspensions. The second reason might be about two different particle size distribution in suspension, and this cause different oscillating-migration behavior under AC-EPD. Therefore, the deposition is the more closed packed structure [10].

After the application of tape-test, coating damage of the samples are classified as 3B for AC-HB 0.0 and AC-HB 2.0, 4B for AC-HB 5.0 and AC-HB 10.0 and 5B for AC-HB 25.0 at 25 Vpp for 2 min (Figure 6). Tape test samples give more objective results about the adhesion of the coating formed by EPD. These results are comply with our assumption. AC-HB25.0 coded samples were good and classified to category 5B according to ASTM standards. The 5B ranking suggests that the HA-hBN nanoparticles coating adhere excellently to the Ti substrate. The peeling of the coating from the surface (less than 5%) was observed in the sample AC-HB 5.0 and AC-HB 10.0 and classified to category 4B. Figure 7 shows the microstructure of composite coatings after tape tests. The crosshatch patterns on samples are seen Figure 7 a, c, e, g and I. The microstructures between crosshatch lines are shown Figure 7 b, d, f, h and j. These results are comply with our assumption.

It was determined boron and nitrogen peaks beside Ca, P and O peaks on AC-HB 10.0 (Figure 8) and AC-HB 25.0 (Figure 9) after tape tests. In order to determine where boron and nitrogen is located in the microstructure, AC-HB 10.0 (Figure 10) and AC-HB 25.0 coated samples (Figure 11) were analyzed by elemental mapping. The elemental mapping analysis of each sample showed that boron and nitrogen distributed on the coating surfaces are uniform.

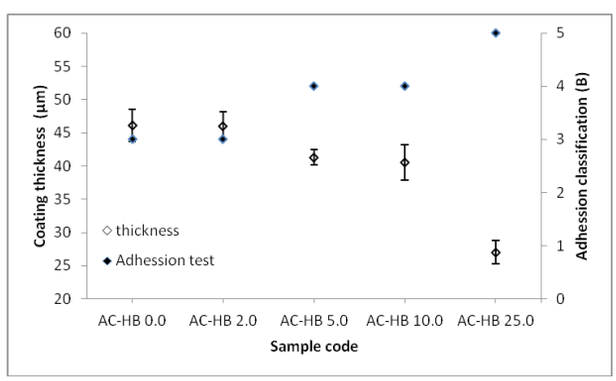

Figure 6. The coating thickness and classification adhesion vs HA-hBN composite samples.

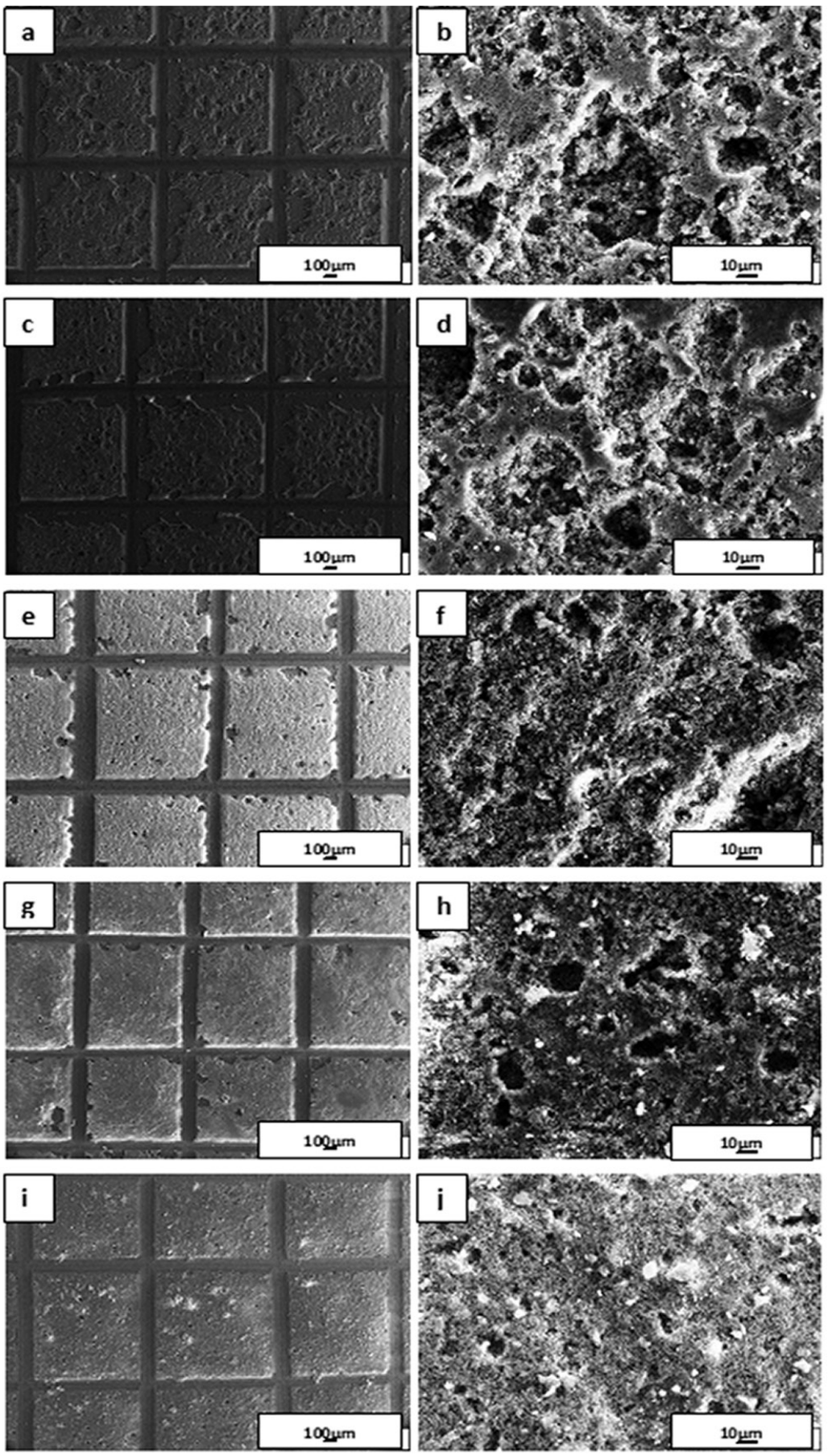

Figure 7. SEM images of HA-hBN composite samples, a, b) AC-HB 0.0; c, d) AC-HB 2.0; e, f) AC-HB 5.0; g, h) AC-HB 10.0; i, j) AC-HB 25.0.

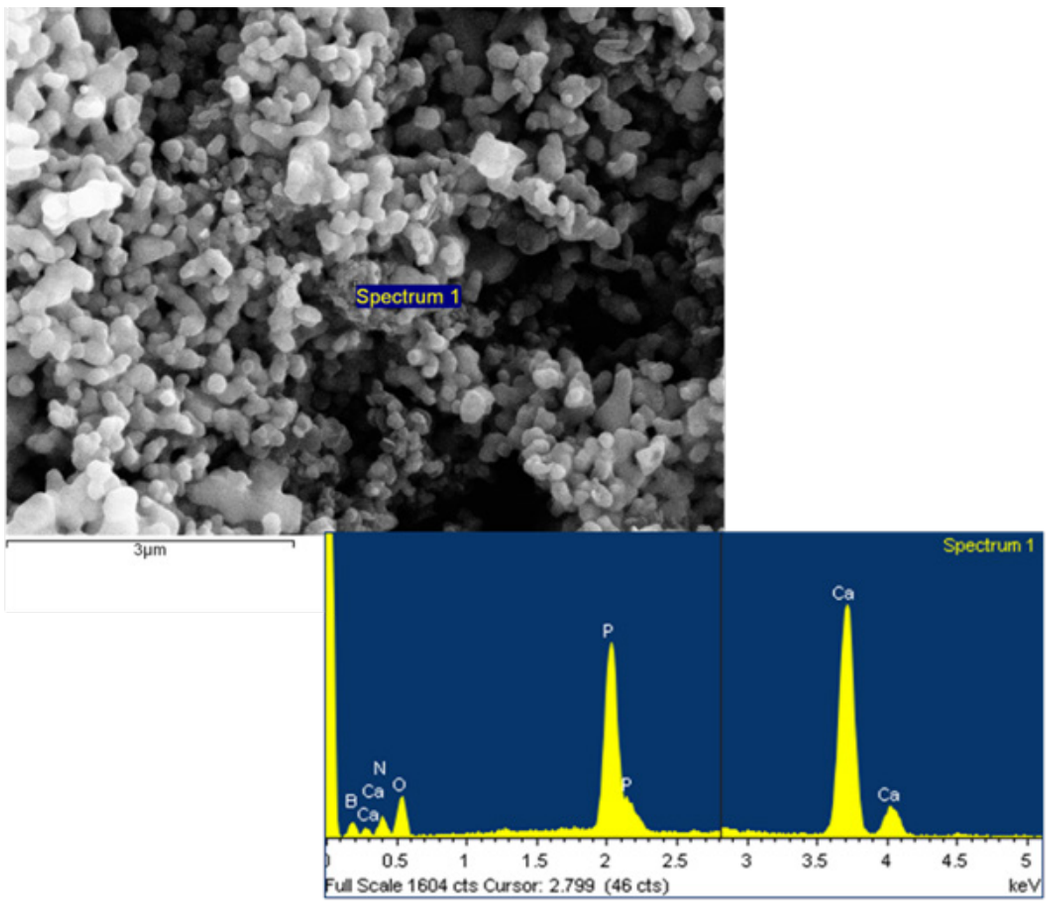

Figure 8. SEM-EDX analysis of AC-HB 10.0 sample.

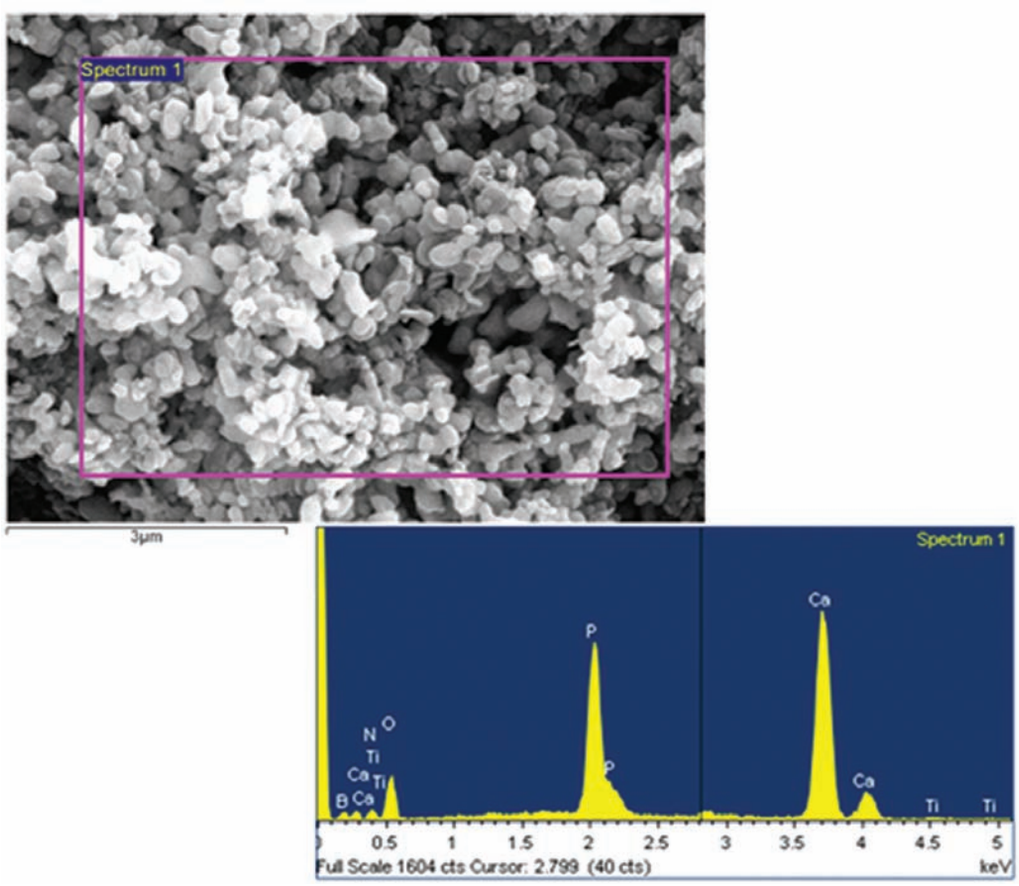

Figure 9. SEM-EDX analysis of AC-HB 25.0 sample.

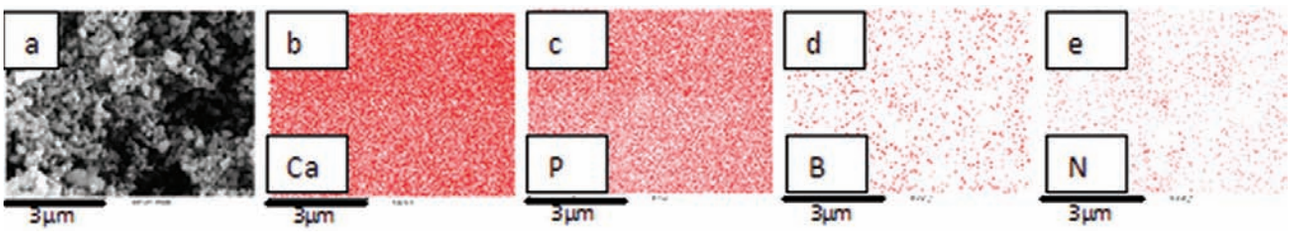

Figure 10. a) Elemental mapping on coating surface of AC-HB 10.0 sample, images (b) – (e) exhibit the element sensitive maps of calcium, phosphorus, boron and nitrogen.

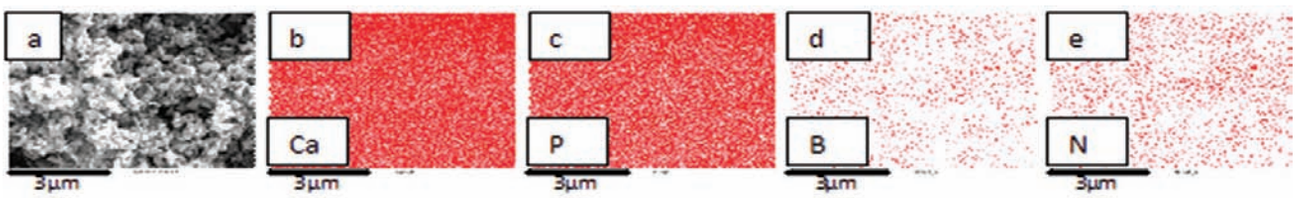

Figure 11. a) Elemental mapping on coating surface of AC-HB 25.0 sample, images (b) – (e) exhibit the element sensitive maps of calcium, phosphorus, boron and nitrogen.

4. Conclusions

In this study, obtained the nano HA-nano hBN composite coating by AC-EPD method are homogeneous and crack free. The results indicate that the coating thickness are required less deposition time with rising applied voltage and also adhesion classification value is decreased with increasing coating thickness. Increasing hBN amount in the composite coating provides less thin coating. It is determined that the amount of hBN in composite affects the thickness of coating and adhesion is rising with increasing hBN amount.

Acknowledgements

This work has been supported by the Scientific and Technological Research Council of Turkey (TUBITAK) National Science Foundation through Grant No: 112M590 and 2211 D- Domestic PhD. Scholarship programme for Industry (2015-1) and Anadolu University Scientific Research Grant No: 1507F564.

References

[1] Park B., Lakes, R.S., Biomaterials: An Introduction, Plenum Press, New York, 1992.

[2] Ravaglioli A., Krajewski A., Bioceramics: Materials, Properties, Applications, Chapman & Hall, London, 1992.

[3] Mavis B., Taş A. C., Dip coating of calcium hydroxyapatite on Ti-6Al-4V substrates, J. Am. Ceram. Soc., 83 (4), 989–991, 2000.

[4] Yu L.G., Khor K. A., LI H., Cheang P., Effect of spark plasma sintering on the microstructure and in vitro behavior of plasma sprayed HA coatings, Biomaterials, 24, 2695-2705, 2013.

[5] Habibovic P., Barre`re F., Blitterswijk C. A. V., Groot K. D., Layrolle P., Biomimetic hydroxyapatite coating on metal implants, J. Am. Ceram. Soc., 85 (3), 517–522, 2002.

[6] Zhitomirsky I., Gal-Or L., Electrophoretic deposition of hydroxyappatite, J. Mater Sci. Mater., Med., 8, 213-219, 1997.

[7] Boccacini A. R., Keim S., Ma, R., Li, Y., Zhitomirsky I., Electrophoretic deposition of biomaterials, J.R, Soc, Interface, 7, 581-613, 2010.

[8] Ammam M., Electrophoretic deposition under modulated electric fields: A Review, RSC Advances, 2, 7633-7646, 2012.

[9] Besra L., Liu M., A review on fundamentals and applications of electrophoretic deposition (EPD), Prog. Mater. Sci., 52, 1-61, 2007.

[10] Ozhukil Kollath V., Chen Q., Closset R., Luyten J., Traina K., Mullens S., Boccaccini A. R., Cloots, R., et al., DC electrophoretic deposition of hydroxyapatite on titanium, J. Eur. Ceram. Soc., 33, 2715–2721, 2013.

[11] Weimer A. W., Carbide, Nitride and Boride Materials Synthesis and Production, Chapman &Hall Pub., London, 1997.

[12] Chen X., Wu P., Rousseas M., Okawa D., Gartner Z., Zettl A. Bertozzi C. R., Boron nitride nanotubes are noncytotoxic and can be functionalized for interaction with proteins and cell, J. Am. Chem. Soc., 131(3), 890-891, 2009.

[13] Ciofani G., Danti S., D'Alessandro D., Moscato S. Menciassi A., Assessing cytotoxicity of boron nitride nanotubes: Interference with the MTT assay, Biochem. Biophys. Res. Commun., 394, 405-411, 2010.

[14] Lahiri D., Rouzaud F., Richard T., Keshri A. K., Bakshi S. R., Kos L. Agarwal A., Boron nitride nanotube reinforced polylactide–polycaprolactone copolymer composite: Mechanical properties and cytocompatibility with osteoblasts and macrophages in vitro, Acta Biomater., 6, 3524-3533, 2010.

[15] Göncü Y., Geçgin M., Baka, F., Ay N., Electrophoretic deposition of hydroxyapatite-hexagonal boron nitride composite coatings on Ti substrate, Mater. Sci. Eng. C, 79, 343–353, 2017.

[16] Lahiri D., Singh V., Benaduc, A. P., Seal S., Kos L., Agarwal A., Boron nitride nanotube reinforced hydroxyapatite composite: Mechanical and tribological perfor-

mance and in-vitro biocompatibility to osteoblasts, J. Mech. Behav. Biomed. Mater., 4, 44-56, 2011.

[17] Prajatelistia E., Han Y. H., Kım B. N, Kim Y. M., Lee K., Jeong Y. K., Kim D.I., et al., Characterization of boron nitride-reinforced hydroxyapatite composites prepared by spark plasma sintering and hot press, J. Ceram. Soc. Jpn, 121(1412), 344-347, 2013.

[18] Topcu A., Halici Z., Karakus E., Cadirci E. Dogan A., Effects of Boron Nitride and/or Hydroxyapatite Compounds on Bone Defect in Osteoporotic Rats, in: J.A. Kanis, R. Linsday (Eds.) Osteoporosis International with other metabolic bone diseases, Springer, Milan Italy, 2015.

[19] Yayla M., Halici Z., Cadirci E., Karakus E., Demirci S., Effects of Boron Nitride and/or Hydroxyapatite Compounds on Bone Formation in Rat Carvarial Defect Model, in: J.A. KANIS, R. LINDSAY (Eds.) Osteoporosis International with other metabolic bone diseases, Springer, Milan Italy, pp. 678, 2015.

[20] Halici Z., Polat B., Karakus E., Bayir Y., Albayrak A., Aydin A., Cadirci E. Ay N., Effects of Boron Nitride and/or Hydroxyapatite Compounds on Bone Defect Model of Rats, in: J.A. KANIS, R. LINDSAY (Eds.) Osteoporosis International with other metabolic bone diseases, Springer, Milan Italy, 2015.

[21] Halici Z., Cadirci E., Karakus E., Bayir Y., Albayrak A., Aydin A., Polat B., Ay N., Effects of Boron Nitride and/or Hydroxyapatite Plaques on Bone Healing in Rats With Femoral Fracture, in: J.A. KANIS, R. LINDSAY (Eds.) Osteoporosis International with other metabolic bone diseases, Springer, Milan Italy, p 683, 2015.

[22] Ferah I., The Effects of Boron Nitride and/or Hydroxyapatite Compounds on Experimentally Induced Osteomyelitis Following Open Femoral Fracture in Rats, Health Sciences Institute, Atatürk University, Erzurum, Turkey, p. 109, 2015.

[23] Atila A., Halici Z., Cadirci E., Karakus E., Palabiyik S. S., Ay N., Bakan F., Yilmaz S., Study of the boron levels in serum after implantation of different ratios nano-hexagonal boron nitride–hydroxy apatite in rat femurs, Mater. Sci. Eng. C, 58, 1082–1089, 2016.

[24] Geçgin M., Alli E., Göncü M., Ay N., The characterization of hydroxyapatite-hexagonal boron nitride composites with forming cold isostatic pressing, The International Porous and Powder Materials Symposium and Exhibition, İzmir, Turkey, 15-18 September, 2015.

[25] Standard Test Methods for Measuring Adhesion by Tape Test, Test Method B—Cross-Cut Tape Test, ASTM D3359-09.

[26] Chávez-Valdez A., Herrmann M., Boccaccini A. R., Alternating current electrophoretic deposition (EPD) of TiO_2 nanoparticles in aqueous suspensions, J. Colloid Interface Sci., 375, 102–105, 2012.

[27] Gardeshzadeh A. R., Raissi B., Merzbanrad E., Electrophoretic deposition of SnO_2 nanoparticles using low frequency AC electric fields, Mater. Lett., 62, 1697–1699, 2008.

[28] Ferrari B., Moreno R., EPD Kinetics: A review, J. Eur. Ceram. Soc., 30, 1069-1078, 2010.

[29] Sarkar N. Nicholso, P. S., Electrophoretic deposition (EPD): Mechanisms, kinetics, and application to ceramics, J. Am. Ceram. Soc., 79 (8), 1987-2002, 1996.

[30] Standard Test Method for Adhesion or Cohesive Strength of Flame-Sprayed Coating, ASTM Standard C633-79.

[31] Standard Test Method for Tension of Porous Metal Coatings, ASTM Standard F1147-88.

[32] Standard Test Method for Shear Strength of Adhesive Bonds between Rigid Substrates by the Block-Shear Method, ASTM Standard D4501-91.

[33] Standard Test Methods for Shear Testing of Porous Metal Coatings, ASTM Standard F1044-87.

[34] Seuss S., Lehmann M., Boccaccini A. R., Alternating current electrophoretic deposition of antibacterial bioactive glass-chitosan composite coatings, Int. J. Mol. Sci., 15, 12231-12242, 2014.

[35] Raddaha N. S., Cordero-Arias L., Cabanas-Polo S., Virtanen S., Roether J. A., Boccaccini A. R., Electrophoretic deposition of chitosan/h-BN and chitosan/h-BN/TiO_2 composite coatings on stainless steel (316L) substrates, Mater., 7, 1814-1829, 2014.

[36] Coan T., Barroso G. S., Motz G., Bolzán A., Machado R. A. F., Preparation of PMMA/hBN composite coatings for metal surface protection, Mater. Res., 16 (6), 1366-1372, 2013.

[37] Wei M., Ruys A. J., Milthorpe B. K., Sorrell C. C., Evans J. H., electrophoretic deposition of hydroxyapatite coatings on metal substrates: A nanoparticulate dual-coating approach, J. Sol-Gel Sci. and Technol., 21, 39–48, 2001.

[38] Wei M., Ruys,A. J., Swain M. V., Milthorpe B. K., Sorrell C. C., Hydroxyapatite-coated metals: Interfacial reactions during sintering,J. mater. Sci.: Mater. Med.,16, 101 – 106, 2005.